arXiv:0804.0341v1 [quant-ph] 2 Apr 2008

Entanglement and Non-locality in a Micro-Macroscopic system

Francesco De Martini[1,2], Fabio Sciarrino [3,1], and Chiara Vitelli[1]
[1] *Dipartimento di Fisica dell'Universitá "La Sapienza" and*
Consorzio Nazionale Interuniversitario per le Scienze Fisiche della Materia,
Roma, 00185 Italy
[2] *Accademia Nazionale dei Lincei, Roma*
[3] *Centro di Studi e Ricerche "Enrico Fermi", Via Panisperna*
89/A,Compendio del Viminale, Roma 00184, Italy

PACS numbers:

In recent years two fundamental aspects of quantum mechanics have attracted a great deal of interest, namely the investigation on the irreducible nonlocal properties of Nature implied by quantum entanglement and the physical realization of the "Schrœdinger Cat". The last concept, by applying the nonlocality property to a combination of a microscopic and of a macroscopic systems, enlightens the concept of the quantum state, the dynamics of large systems and ventures into the most intriguing philosophical problem, i.e. the emergence of quantum mechanics in the real life. Rather surprisingly these two aspects, which appeared in the same year 1935 by the separated efforts of Albert Einstein, Boris Podolsky and Nathan Rosen (EPR) and of Erwin Schrœdinger [1, 2] appear not being generally appreciated for their profound interconnections that establish the basic foundations of modern science. Likely, this follows from the extreme difficulty of realizing a system which realizes simultaneously the following three conditions: (a) the quantum superposition of two multiparticle, mutually orthogonal states, call it a "Macro-system" (b) the quantum non-separability of this superposition with a far apart single-particle state, i.e. the "Micro-system", (c) the violation of the Bell's inequality stating that by no means any hidden variable formulation can simulate the nonlocal correlations affecting the joint Micro-Macro system [3].

In the present work these crucial conditions are simultaneously realized and experimentally tested. A Macro - state consisting of N $\approx 3.5\times10^4$ photons in a quantum superposition and entangled with a far apart single - photon state is generated. Then, the non-separability of the overall Micro-Macro system is demonstrated and the corresponding Bell's inequalities are found to be violated. Precisely, an entangled photon pair is created by a nonlinear optical process, then one photon of the pair is injected into an optical parametric amplifier (OPA) operating for any input polarization state, i.e. into a phase-covariant cloning machine. Such transformation establishes a connection between the single photon and the multi particle fields, as show in Figure 1. We then demonstrate the non-separability of the bipartite system by adopting a local filtering technique within a positive operator valued measurement (POVM) [4]. The work shows that the amplification process applied to a microscopic system is a natural approach to enlighten the quantum-to-classical transition and to investigate the persistence of quantum phenomena into the "classical" domain by measurement procedures applied to quantum systems of increasing size [5]. Furthermore, since the generated Micro-Macro entangled state is directly accessible at the output of the apparatus, the implementation of significant multi qubit logic gates for quantum information technology can be achieved by this method. At last, we demonstrate how our scheme may be up-graded to an entangled Macro - Macro quantum system, by then establishing a peculiar nonlocal correlation process between two space-like separated macroscopic quantum superpositions.

In recent years quantum entanglement has been demonstrated within a two photon system [6], within a single trapped-ion one-photon system [7, 8], within a single photon and atomic ensemble [9, 10], within atomic ensembles [11, 12, 13, 14, 15] and superconducting qubits [16]. In addition, the observation of quantum features has been extended to "cluster" entangled states involving four [17], five [18]and six particles [19, 20] and to a more complex architecture [21].

The innovative character of the present work is enlightened by the diagrams reported in Figure 1. While, according to the 1935 proposal the nonlocal correlations were conceived to connect the dynamics of two "microscopic" objects, i.e. two spins within the well known EPR-Bohm scheme here represented by diagram (a)[6], in the present work the entanglement is established between a "microscopic" and a "macroscopic", i.e. multiparticle quantum object, via cloning amplification: diagram (b). The amplification is achieved by adopting a high-gain nonlinear (NL) parametric amplifier acting on a single-photon input carrier of quantum information, i.e., a qubit state: $|\phi\rangle$. This process, referred to as "quantum injected optical parametric amplification"

(QI-OPA) [4, 22] turned out to be particularly fruitful in the recent past to gain insight into several little explored albeit fundamental, modern aspects of quantum information, as quantum cloning machines [4, 23, 24], quantum U-NOT gate [25], quantum no-signaling [26]. Here, by exploiting the amplification process, we convert a single photon qubit into a Macro-qubit involving a large number of photons. Let us venture in a more detailed account of our endeavor.

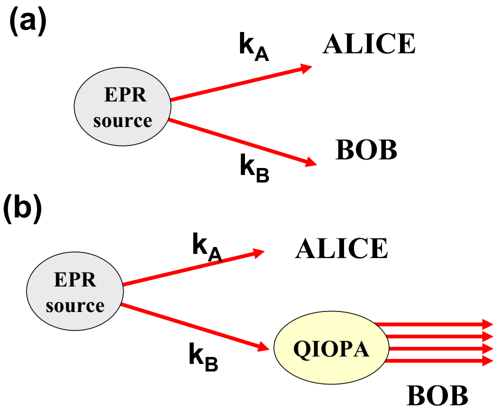

FIG. 1: (a) Generation of an entangled photon pair by Spontaneous Parametric Down Conversion (SPDC) in a nonlinear (NL) crystal; (b) Schematic diagram showing the single photon Quantum-Injected Optical Parametric Amplification (QI-OPA).

I. TEST OF MICRO-MACRO ENTANGLEMENT

An entangled pair of two photons in the singlet state $|\Psi^{-}\rangle_{A,B}$=$2^{-\frac{1}{2}}\left(|H\rangle_A|V\rangle_B - |V\rangle_A|H\rangle_B\right)$ was produced through a Spontaneous Parametric Down-Conversion (SPDC) by the NL crystal 1 (C1) pumped by a pulsed UV pump beam: Fig.2. There $|H\rangle$ and $|V\rangle$ stands, respectively, for a single photon with horizontal and vertical polarization while the labels A, B refer to particles associated respectively with the spatial modes $\mathbf{k}_A$and $\mathbf{k}_B$. Precisely, A, B represent the two space-like separated Hilbert spaces coupled by the entanglement. The photon belonging to $\mathbf{k}_B$, together with a strong ultraviolet (UV) pump laser beam, was fed into an optical parametric amplifier consisting of a NL crystal 2 (C2) pumped by the beam $\mathbf{k}'_P$. More details on this setup and on its properties are given in the Appendix and in [27]. The crystal 2, cut for collinear operation, emitted over the two modes of linear polarization, respectively horizontal and vertical associated with $\mathbf{k}_B$. The interaction Hamiltonian of the parametric amplification $\widehat{H} = i\chi\hbar\widehat{a}^{\dagger}_{H}\widehat{a}^{\dagger}_{V} + h.c.$ acts on the single spatial mode $\mathbf{k}_B$ where $\widehat{a}^{\dagger}_{\pi}$ is the one photon creation operator associated with the polarization $\overrightarrow{\pi}$. The main feature of this Hamiltonian is its property of "phase-covariance" for "equatorial" qubits $|\phi\rangle$, i.e. representing equatorial states of polarization, $\overrightarrow{\pi}_{\phi} = 2^{-1/2}\left(\overrightarrow{\pi}_H + e^{i\phi}\overrightarrow{\pi}_V\right), \overrightarrow{\pi}_{\phi\perp} = \overrightarrow{\pi}^{\perp}_{\phi}$, in a Poincaré sphere representation having $\overrightarrow{\pi}_H$ and $\overrightarrow{\pi}_V$ as the opposite "poles" [27]. The equatorial qubits are expressed in terms of a single phase $\phi \in (0, 2\pi)$ in the basis $\{|H\rangle, |V\rangle\}$. Owing to the corresponding invariance under $U(1)$ transformations, we can then rewrite: $\widehat{H} = \frac{1}{2}i\chi\hbar e^{-i\phi}\left(\widehat{a}^{\dagger 2}_{\phi} - e^{i2\phi}\widehat{a}^{\dagger 2}_{\phi\perp}\right) + h.c.$ where $\widehat{a}^{\dagger}_{\phi} = 2^{-1/2}(\widehat{a}^{\dagger}_{H} + e^{i\phi}\widehat{a}^{\dagger}_{V})$ and $\widehat{a}^{\dagger}_{\phi\perp} = 2^{-1/2}(-e^{-i\phi}\widehat{a}^{\dagger}_{H} + \widehat{a}^{\dagger}_{V})$. The generic polarization state of the injected photon $|\psi\rangle_B$state on mode $\mathbf{k}_B$ evolves into the output state $\left|\Phi^{\psi}\right\rangle_B = \widehat{U}|\psi\rangle_B$ according to the OPA unitary transformation $\widehat{U}$ [27]. The overall output state amplified by the OPA apparatus is expressed, in any polarization equatorial basis $\{\overrightarrow{\pi}_{\phi}, \overrightarrow{\pi}_{\phi\perp}\}$, by the Micro-Macro entangled state commonly referred to in the literature as the "Schroedinger Cat State" [28]

$$|\Sigma\rangle_{A,B} = 2^{-1/2}\left(\left|\Phi^{\phi}\right\rangle_B\left|1\phi^{\perp}\right\rangle_A - \left|\Phi^{\phi\perp}\right\rangle_B|1\phi\rangle_A\right) \quad (1)$$

where the mutually orthogonal multi-particle "Macro-states" are:

$$\left|\Phi^{\phi}\right\rangle_B = \sum_{i,j=0}^{\infty}\gamma_{ij}\frac{\sqrt{(1+2i)!(2j)!}}{i!j!}\left|(2i+1)\phi;(2j)\phi^{\perp}\right\rangle_B \quad (2)$$

$$\left|\Phi^{\phi\perp}\right\rangle_B = \sum_{i,j=0}^{\infty}\gamma_{ij}\frac{\sqrt{(1+2i)!(2j)!}}{i!j!}\left|(2j)\phi;(2i+1)\phi^{\perp}\right\rangle_B \quad (3)$$

with $\gamma_{ij} \equiv C^{-2}(-\frac{\Gamma}{2})^{i}\frac{\Gamma}{2}^{j}$, $C \equiv \cosh g$, $\Gamma \equiv \tanh g$, being g the NL gain [25]. There $\left|p\phi;q\phi^{\perp}\right\rangle_B$ stands for a Fock state with p photons with polarization $\overrightarrow{\pi}_{\phi}$ and q photons with $\overrightarrow{\pi}_{\phi\perp}$ over the mode $\mathbf{k}_B$. Most important, any injected single-particle qubit $(\alpha|\phi\rangle_B + \beta\left|\phi^{\perp}\right\rangle_B)$ is transformed by the *information preserving* QI-OPA operation into a corresponding Macro-qubit $(\alpha\left|\Phi^{\phi}\right\rangle_B + \beta\left|\Phi^{\phi\perp}\right\rangle_B)$, i.e. a "Schrœdinger Cat" like, macroscopic quantum superposition [22]. The quantum states of Eq.(2-3) deserve some comments. The multi-particle states $\left|\Phi^{\phi}\right\rangle_B$, $\left|\Phi^{\phi\perp}\right\rangle_B$ are orthonormal and exhibit observables bearing macroscopically distinct average values. Precisely, for the polarization mode $\overrightarrow{\pi}_{\phi}$ the average number of photons is $\overline{m} = \sinh^2 g$ for $\left|\Phi^{\phi\perp}\right\rangle_B$, and $(3\overline{m}+1)$ for $\left|\Phi^{\phi}\right\rangle_B$. For the $\pi-$mode $\overrightarrow{\pi}_{\phi\perp}$ these values are interchanged among the two Macro-states. On the other hand, as shown by [22], by changing the representation basis from $\{\overrightarrow{\pi}_{\phi}, \overrightarrow{\pi}_{\phi\perp}\}$ to $\{\overrightarrow{\pi}_H, \overrightarrow{\pi}_V\}$, the same Macro-states, $\left|\Phi^{\phi}\right\rangle_B$ or $\left|\Phi^{\phi\perp}\right\rangle_B$ are found to be quantum superpositions of two orthogonal states $\left|\Phi^{H}\right\rangle_B$, $\left|\Phi^{V}\right\rangle_B$ which differ by a single quantum. This unexpected and quite peculiar combination, i.e. a large difference of a measured observable when the states are expressed in one basis and a small Hilbert-Schmidt distance of the same states when expressed in another basis turned out to be a useful and lucky property since it rendered the coherence patterns of our system very robust toward coupling with environment, e.g. losses. This was verified experimentally. The decoherence of our system was investigated experimentally and theoretically in the laboratory: cfr: [24, 27, 29]. The above features are not present in atomic ensemble experiments, in which quantum phenomena usually involve microscopic fluctuations of a macroscopic system and the qubit states are encoded as collective spin excitations.

As shown in Figure 2, the single particle field on mode $\mathbf{k}_A$ was analyzed in polarization through a Babinet-Soleil phase-shifter (PS), i.e. a variable birefringent optical retarder, two waveplates $\left\{\frac{\lambda}{4}, \frac{\lambda}{2}\right\}$ and polarizing beam splitter (PBS). It was finally detected by two single-photon detectors D_A and D_A^* (ALICE box). The multiphoton QI-OPA amplified field associated with the mode $\mathbf{k}_B$ was sent, through a single-mode optical fiber (SM), to a measurement apparatus consisting of a set of waveplates $\left\{\frac{\lambda}{4}, \frac{\lambda}{2}\right\}$, a (PBS) and two photomultipliers (PM) P_B and P_B^* (BOB box). The output signals of the PM's were analyzed by an "orthogonality filter" (OF) that will be described shortly in this paper.

We now investigate the bipartite entanglement between the modes $\mathbf{k}_A$ and $\mathbf{k}_B$. We define the $\frac{1}{2}-$spin Pauli operators $\{\hat{\sigma}_i\}$ for a single photon polarization state, where the label $i = (1,2,3)$ refer to the polarization bases: $i = 1 \Longleftrightarrow \{\overrightarrow{\pi}_H, \overrightarrow{\pi}_V\}$, $i = 2 \Longleftrightarrow \{\overrightarrow{\pi}_R, \overrightarrow{\pi}_L\}$, $i = 3 \Longleftrightarrow \{\overrightarrow{\pi}_+, \overrightarrow{\pi}_-\}$. Here $\overrightarrow{\pi}_R = 2^{-1/2}(\overrightarrow{\pi}_H - i\overrightarrow{\pi}_V), \overrightarrow{\pi}_L = \overrightarrow{\pi}_R^{\perp}$ are the right and left handed circular polarizations and $\overrightarrow{\pi}_\pm = 2^{-1/2}(\overrightarrow{\pi}_H \pm \overrightarrow{\pi}_V)$. It is found $\hat{\sigma}_i = \left|\psi_i\right\rangle\left\langle\psi_i\right| - \left|\psi_i^\perp\right\rangle\left\langle\psi_i^\perp\right|$ where $\left\{\left|\psi_i\right\rangle, \left|\psi_i^\perp\right\rangle\right\}$ are the two orthogonal qubits corresponding to the $\overrightarrow{\pi}_i$ basis, e.g., $\left\{\left|\psi_1\right\rangle, \left|\psi_1^\perp\right\rangle\right\} = \{\left|H\right\rangle, \left|V\right\rangle\}$, etc. By the QI-OPA unitary process the single-photon $\hat{\sigma}_i$ operators evolve into the "Macro-spin" operators: $\hat{\Sigma}_i = \hat{U}\hat{\sigma}_i\hat{U}^\dagger = \left|\Phi^{\psi i}\right\rangle\left\langle\Phi^{\psi i}\right| - \left|\Phi^{\psi i\perp}\right\rangle\left\langle\Phi^{\psi i\perp}\right|$. Since the operators $\left\{\hat{\Sigma}_i\right\}$ are built from the unitary evolution of eigenstates of $\hat{\sigma}_i$, they satisfy the same commutation rules of the single particle $\frac{1}{2}-$spin: $\left[\hat{\Sigma}_i, \hat{\Sigma}_j\right] = \varepsilon_{ijk}2i\hat{\Sigma}_k$ where ε_{ijk} is the Levi-Civita tensor density. The generic state $(\alpha\left|\Phi^H\right\rangle_B + \beta\left|\Phi^V\right\rangle_B)$ is a Macro-qubit in the Hilbert space B spanned by $\left\{\left|\Phi^H\right\rangle_B, \left|\Phi^V\right\rangle_B\right\}$, as said. To test whether the overall output state is entangled, one should measure the correlation between the single photon spin operator $\hat{\sigma}_i^A$ on the mode $\mathbf{k}_A$ and the Macro-spin operator $\widehat{\Sigma}_i^B$ on the mode $\mathbf{k}_B$. We then adopt the criteria for two qubit bipartite systems based on the spin-correlation. We define the "visibility" $V_i = \left|\left\langle\widehat{\Sigma}_i^B \otimes \widehat{\sigma}_i^A\right\rangle\right|$ a parameter which quantifies the correlation between the systems A and B. Precisely $V_i = \left|P(\psi_i, \Phi^{\psi i}) + P(\psi_i^\perp, \Phi^{\psi i\perp}) - P(\psi_i, \Phi^{\psi i\perp}) - P(\psi_i^\perp, \Phi^{\psi i})\right|$ where $P(\psi_i, \Phi^{\psi i})$ is the probability to detect the systems A and B in the states $\left|\psi_i\right\rangle_A$ and $\left|\Phi^{\psi i}\right\rangle_B$, respectively. The value $V_i = 1$ corresponds to perfect anti-correlation, while $V_i = 0$ expresses the absence of any correlation. The following upper bound criterion for a separable state holds [30]:

$$S = (V_1 + V_2 + V_3) \leq 1 \tag{4}$$

In order to measure the expectation value of $\widehat{\Sigma}_i^B$ a discrimination among the pair of states $\left\{\left|\Phi^{\psi i}\right\rangle_B, \left|\Phi^{\psi i\perp}\right\rangle_B\right\}$ for the three different polarization bases $1,2,3$ is required. Consider the Macro-states $\left|\Phi^+\right\rangle_B$, $\left|\Phi^-\right\rangle_B$ expressed by Equations 2-3, for $\phi = 0$ and $\phi = \pi$. In principle, a perfect discrimination can be achieved by identifying whether the number of photons over the $\mathbf{k}_B$ mode with polarization $\overrightarrow{\pi}_+$ is even or odd, i.e. by measuring an appropriate "parity operator". This requires the detection of the macroscopic field by a perfect *photon-number resolving* detectors operating with an overall quantum efficiency $\eta \approx 1$, a device out of reach of the present technology.

It is nevertheless possible to exploit, by a somewhat sophisticated electronic device dubbed "Orthogonality Filter" (OF), the macroscopic difference existing between the functional characteristics of the probability distributions of the photon numbers associated with the quantum states $\{\left|\Phi^\pm\right\rangle_B\}$. The measurement scheme works as follows: Figures 2 and 3. The multiphoton field is detected by two PM's (P_B, P_B^*) which provide the electronic signals (I_+, I_-) corresponding to the field intensity on the mode $\mathbf{k}_B$ associated with the $\pi-$components $(\overrightarrow{\pi}_+, \overrightarrow{\pi}_-)$, respectively. By (OF) the difference signals $\pm(I_+ - I_-)$ are compared with a threshold $\xi k > 0$. When the condition $(I_+ - I_-) > \xi k$ $((I_- - I_+) > \xi k)$ is satisfied, the detection of the state $\left|\Phi^+\right\rangle_B$ $(\left|\Phi^-\right\rangle_B)$ is inferred and a standard transistor-transistor-logic (TTL) electronic square-pulse L_B (L_B^*) is realized at one of the two output ports of (OF). The PM output signals are discarded for $-\xi k < (I_+ - I_-) < \xi k$, i.e. in condition of low state discrimination. By increasing the value of the threshold k an increasingly better discrimination is obtained together with a decrease of detection efficiency. This "local distillation" procedure is conceptually justified by the following theorem: since entanglement cannot be created or enhanced by any "local" manipulation of the quantum state, the non-separability condition demonstrated for a "distilled" quantum system, e.g., after application of the OF-filtering procedure, fully applies to the same system in absence of distillation [30]. This statement can be applied to the measurement of I_ϕ and $I_{\phi\perp}$ for any pair of quantum states $\left\{\left|\Phi^\phi\right\rangle_B, \left|\Phi^{\phi\perp}\right\rangle_B\right\}$. This method is but an application of a Positive Operator Value Measurement procedure (POVM) [31] by which a large discrimination between the two states $\{\left|\Phi^\pm\right\rangle_B\}$ is attained at the cost of a reduced probability of a successful detection. A detailed description of the OF device and of its properties is found in the Appendix and in Ref.[27].

The present experiment was carried out with a gain value $g = 4.4$ leading to a number of output photons $N \approx 3 \times 10^4$, after OF filtering. In this case the probability of photon transmission through the OF filter was: $p \approx 10^{-4}$. A NL gain $g = 6$ was also achieved with no substantial changes of the apparatus. Indeed, an unlim-

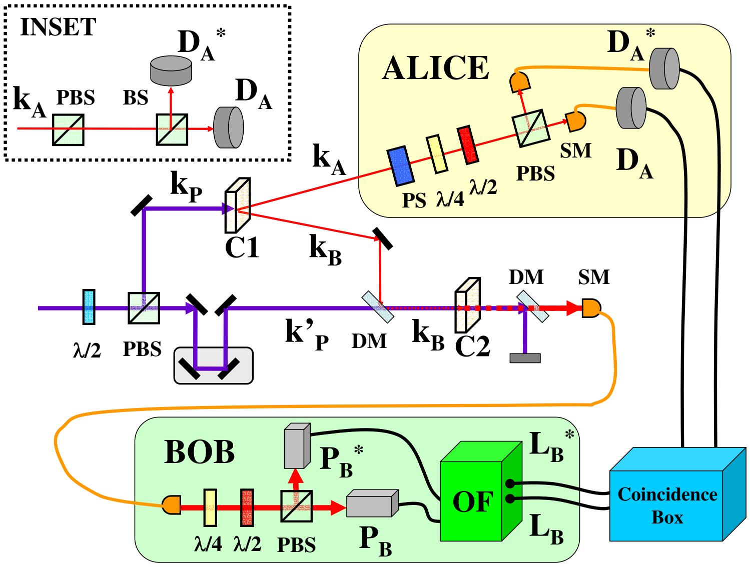

FIG. 2: Optical configuration of the QI-OPA apparatus. The SPDC quantum injector (NL crystal 1: C1) is provided by a type II generator of polarization-entangled photon couples. C1 generates an average photon number per mode equal to about 0.35, while the overall detection efficiency of the trigger mode was estimated to be $\simeq 10\%$. The NL crystal 2: C2, realizing the optical parametric amplification (OPA), is cut for collinear type II phase matching. Both crystals C1 and C2 are 1.5 mm thick. The fields are coupled to single mode (SM) fibers. INSET: Two photon $\pi-$states over the mode $\mathbf{k}_A$ are detected through a fiber coupled beam-splitter BS by a pair of single-photon detectors D_A and D_A^*. A coincidence device, not shown in the Figure reveals a coincidence between two simultaneous detection events by D_A and D_A^* with the emission of a transistor-transistor logic (TTL) square signal $\overline{D_A}$. For the amplification of the 2-photon state, the intensity of the UV pump laser beam $\mathbf{k}_P$ was set at a level apt to generate 3 pairs of photons in the NL crystal 1 with a low probability: $p \sim 0.10$.

ited number of photons could be generated in principle by the QI-OPA technique, the only limitation being due to the fracture of the NL crystal 2 in the focal region of the laser pump. In order to verify the correlations existing between the single photon generated by the NL crystal 1 and the corresponding amplified Macro-state, we have recorded the coincidences between the single photon detector signal D_A (or D_A^*) and the TTL signal L_B (or L_B^*) both detected in the same $\pi-$basis $\{\overrightarrow{\pi}_+, \overrightarrow{\pi}_-\}$: Figure 2. This measurement has been repeated by adopting the common basis $\{\overrightarrow{\pi}_R, \overrightarrow{\pi_L}\}$.

Since the filtering technique can hardly be applied to the $\{\overrightarrow{\pi}_H, \overrightarrow{\pi}_V\}$ basis, because of the lack of a broader $SU(2)$ covariance of the amplifier, the small quantity $V_1 > 0$ could not be precisely measured. The phase ϕ between the $\pi-$components $\overrightarrow{\pi}_H$ and $\overrightarrow{\pi}_V$ on mode $\mathbf{k}_A$ was determined by the Babinet-Soleil variable phase shifter (PS). Figure 4 shows the fringe patterns obtained by recording the rate of coincidences of the signals detected by the Alice's and Bob's measurement apparata, for different values of ϕ. These patterns were obtained by adopting the common analysis basis $\{\overrightarrow{\pi}_R, \overrightarrow{\pi}_L\}$ with a filtering probability $\simeq 10^{-4}$, corresponding to a threshold ξk about 8 times higher than the average photomultiplier signals I. In this case the average visibility has been found $V_2 = (54.0 \pm 0.7)\%$. A similar oscillation pattern has been obtained in the basis $\{\overrightarrow{\pi}_+, \overrightarrow{\pi}_-\}$ leading to: $V_3 = (55 \pm 1)\,\%$. Since always is $V_1 > 0$, our experimental result $S = V_2 + V_3 = (109.0 \pm 1.2)\%$ implies the violation of the separability criteria of Equation (4) and then demonstrates the non-separability of our Micro-Macro system belonging to the space-like separated Hilbert spaces A and B. By evaluating the experimental value of the "concurrence" for our test, connected with the "entanglement of formation", it is obtained $C \geq 0.10 \pm 0.02 > 0$ [32, 33]. This result again confirms the non-separability of our bipartite system. Further details on the measurement can be found in the Appendix. A method similar to ours to test the non-separability of a 2-atom bi-partite system was adopted recently by [14].

II. VIOLATION OF THE MICRO-MACRO BELL'S INEQUALITIES

A further investigation on the persistence of quantum effects in large multi-particle systems has been carried out by performing a nonlocality test implying the violation of a Bell's inequality [34]. To carry out such a test higher correlations among the fields realized on the $\mathbf{k}_A$ and $\mathbf{k}_B$ modes are required. Hence we adopted the QI-OPA amplification of a 4-photon entangled state. In

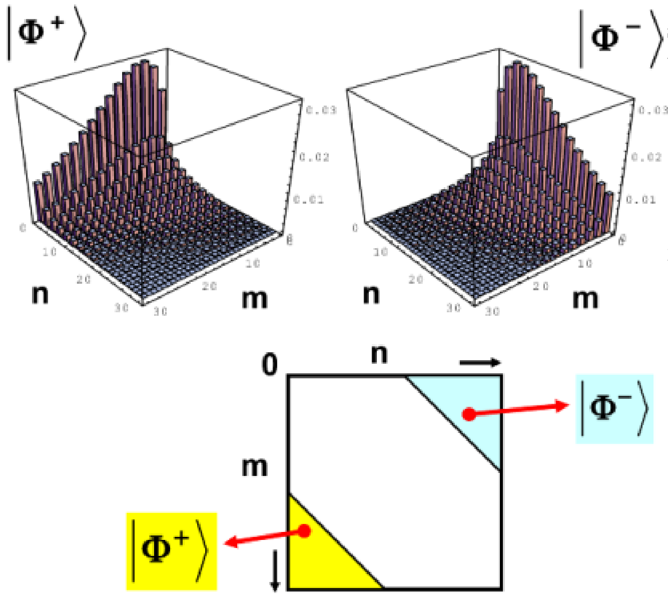

FIG. 3: Theoretical probability distributions $P^{\pm}(m,n)$ of the number of photons associated with the Macro-states $\left|\Phi^{\pm}\right\rangle$ $(g=1.6)$. Probabilistic identification of the wavefunctions $\left|\Phi^{\pm}\right\rangle$ by OF-filtering the $P^{\pm}(m,n)$ distributions over the photon number two-dimensional space $\{m,n\}$. The white section in the cartesian plane (m,n) corresponds to the "inconclusive events" of our POVM OF-filtering technique.

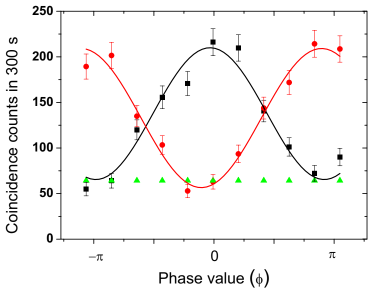

FIG. 4: Coincidence counts versus the phase ϕ of the injected qubit for a common basis $\{\vec{\pi}_+, \vec{\pi}_-\}$: square data $[L_B, D_A]$, circle data $[L_B^*, D_A]$. The "Visibility" of the fringe pattern is: $V \simeq 55\%$. Triangle data: noise due to accidental coincidences.

this second experiment, the NL crystal 1 generated by SPDC two simultaneous entangled photon couples, i.e. a 4-photon entangled state . The 4 photons were emitted over the two output modes $\mathbf{k}_i$ $(i=A,B)$ in the *singlet* state of two spin-1 subsystems

$$|\Psi_2^-\rangle_{AB} = \frac{1}{\sqrt{3}}(|2H\rangle_A|2V\rangle_B - |H;V\rangle_A|H;V\rangle_B + |2V\rangle_A|2H\rangle_B) \tag{5}$$

We note that the state $|\Psi_2^-\rangle_{AB}$ keeps the same expression in any polarization basis owing to its rotational invariance. The 2 photons generated over the mode $\mathbf{k}_B$ were injected into the collinear QI-OPA amplifier: Figure 2. After the amplification process the overall output state can be expressed in any "equatorial" polarization basis $\left\{\overrightarrow{\pi}_\phi, \overrightarrow{\pi}_\phi^\perp\right\}$ on the Poincaré sphere as

$$|\Omega\rangle_{AB} = \frac{1}{\sqrt{3}}\left(|2\phi\rangle_A \left|\Phi^{2\phi^\perp}\right\rangle_B - |\phi;\phi^\perp\rangle_A \left|\Phi^{\phi,\phi^\perp}\right\rangle_B + |2\phi^\perp\rangle_A \left|\Phi^{2\phi}\right\rangle_B\right) \tag{6}$$

where $\left|\Phi^{\psi}\right\rangle_B$ stands for the amplified field generated by injecting the 2-photon state $|\psi\rangle_B$: $\left|\Phi^{\psi}\right\rangle_B = \widehat{U}\,|\psi\rangle_B$.

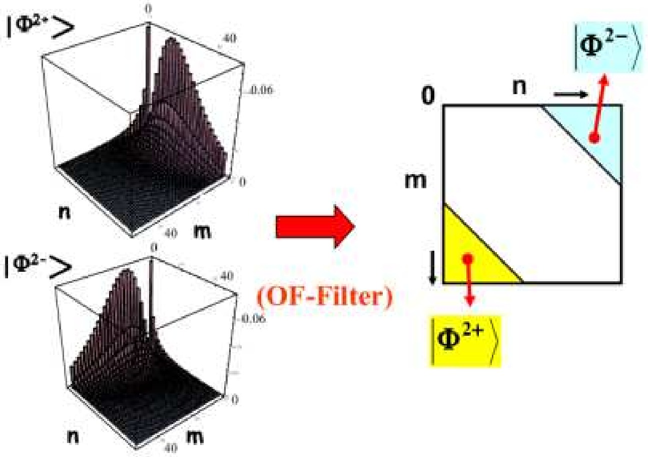

FIG. 5: Theoretical probability distribution $P^{\pm}(m,n)$ of the number of photons associated with the Macro-states $\left|\Phi^{2\pm}\right\rangle$ $(g=1.6)$. Probabilistic identification of wavefunctions $\left|\Phi^{2\pm}\right\rangle$ by OF-filtering the $P^{\pm}(m,n)$ distributions over the photon number two-dimensional space $\{m,n\}$.

Let us analyze the output field when the state $\left|2\phi^\perp\right\rangle_A$ was detected over the mode $\mathbf{k}_A$. This was done by the simultaneous measurement, by the single-photon detectors D_A and D_A^* inserted on the two output modes of an ordinary beam-splitter (BS), of two photons emerging simultaneously from the same output port of a $\pi-$analyzer (PBS), inserted on the mode $\mathbf{k}_A$ (see Figure 2-inset). Each event of simultaneous detection by D_A and $D_A^*$was identified by the generation of a signal $\overline{D_A}$ at the output port of an additional electronic coincidence device, not shown in Figure 2. In this condition the corresponding, correlated state $|2\phi\rangle_B$ was injected into the QI-OPA amplifier on mode $\mathbf{k}_B$ leading to the generation of $\left|\Phi^{2\phi}\right\rangle_B$. When detected in the polarization basis $\overrightarrow{\pi}_\pm$ of the mode $\mathbf{k}_B$, the average photon number $N_\pm$ was found to depend on the phase ϕ as follows: $N_\pm(\phi) = \overline{m} + (5\overline{m}+2)\cos^2\left(\frac{\phi}{2}\right)$ with $\overline{m} = \sinh^2 g$. Hence the output state analyzed in the polarization basis $\overrightarrow{\pi}_\pm$ exhibits a fringe pattern of the field intensity depending on ϕ with a gain-dependent visibility $V_{th} = (4\overline{m}+1)/(6\overline{m}+2)$.When $\phi = 0$, the mode $\overrightarrow{\pi}_+$ is injected by a two photon state, the output field is $\left|\Phi^{2+}\right\rangle_B$ and $N_+(0) = 5\overline{m} + 2$. When $\phi = \pi$, the state $\left|\Phi^{2-}\right\rangle_B$ is generated and a regime of spontaneous emission is established: $N_+(\pi) = \overline{m}$. The two Macro-states $\left\{\left|\Phi^{2\pm}\right\rangle_B\right\}$ were singled out, in our conditional experiment, by the simultaneous detection by the Alice's Measurement apparatus of the correlated states $\left|2\pm\right\rangle_A$. As said, the realization of the state $\left|2\phi\right\rangle_A$ was identified by the emission of the signal $\overline{D_A}$, having previously set the variable phase-shifter PS at the wanted phase value ϕ. The Macro-states $|\Phi^{2\pm}\rangle_B$ exhibited observables macroscopically distinct, the difference being larger than the one observed in the case of the QI-OPA amplification of a single photon state. Accordingly, the $\left\{\left|\Phi^{2\pm}\right\rangle_B\right\}$ state distinguishability problem was found easier than in the single photon case because of a lower mutual overlap of the 2-photon probability distributions. The number of photons emitted by QI-OPA in this experiment, after OF filtering, was $N \approx 3.5 \times 10^4$, with a corresponding transmission probability through the OF filter: $p \approx 10^{-3}$.

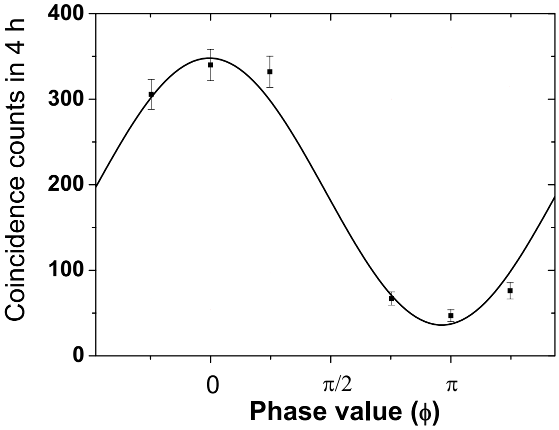

FIG. 6: Coincidence counts $[L_B, \overline{D_A}]$ versus the phase ϕ of the injected ”equatorial”qubit. ”Visibility” of the fringe pattern $V \simeq 81\%$.

We address now the problem of the distinguishability between $\left|\Phi^{2+}\right\rangle_B$ and $\left|\Phi^{2-}\right\rangle_B$, which are mutually orthogonal as shown by the quantum analysis reported in the Appendix. Figure 5 reports the 3-dimensional representations of the two probability distributions of the number of photons which are associated with the two Macro-states $\left|\Phi^{2\pm}\right\rangle_B$. These distributions are drawn as functions of the variables m and n which are proportional to the size of the electronic signals $I_+ = \xi m$ and $I_- = \xi n$ generated by the PM's (P_B, P_B^*). In analogy with the entanglement experiment accounted for in the previous section, a large discrimination between $\left\{\left|\Phi^{2\pm}\right\rangle_B\right\}$ could be obtained by adopting the OF-filter. The output stations located in spaces A and B measured a dichotomic variable with eigenvalues ±1. The correlation fringe patterns reported in Figure 6 were determined by simultaneous detection on the mode $\mathbf{k}_A$ of the state $\left|2\phi\right\rangle_A$ for different values of the ”equatorial” phase ϕ and on the mode $\mathbf{k}_B$ of the OF-filtered $\left\{\left|\Phi^{2\pm}\right\rangle_B\right\}$. Precisely, this was done by recording via the ”Coincidence Box” the rate of coincidences between the signal $\overline{D_A}$ realized at Alice's site and the TTL signal realized at one of the output ports of the OF-filter: Figure 2. The best-fit fringe pattern reported in Figure 6 was obtained by recording, for different ϕ values the coincidence rate between $\overline{D_A}$ and the TTL signal realized at the output port L_B of the OF-filter with a filtering probability $p \approx 10^{-3}$. The visibility of the fringe pattern was found $V = (81 \pm 2)\%$, i.e. a large enough value that allows a Micro-Macro non locality test for the entangled two spin-1 system. An identical but complementary pattern, i.e. shifted by a phase $\phi = \pi$, was found by collecting the coincidences between $\overline{D_A}$ and the TTL realized at the port L_B^* of the OF-filter. This additional pattern is not shown in Fig. 6.

Let us briefly outline the inequality introduced by Clauser, Horne, Shimony, and Holt (CHSH) [3]. Each of two partners, A (Alice) and B (Bob) measures a dichotomic observable among two possible ones, i.e. Alice randomly measures either $\mathbf{a}$ or $\mathbf{a}'$ while Bob measures $\mathbf{b}$ or $\mathbf{b}'$: Figure 7-**a.** For any couple of measured observables ($A = \{\mathbf{a}, \mathbf{a}'\}$, $B = \{\mathbf{b}, \mathbf{b}'\}$), we define the following correlation function

$$E(A,B) = \frac{N(+,+) + N(-,-) - N(+,-) - N(-,+)}{N(+,+) + N(-,-) + N(+,-) + N(-,+)} \tag{7}$$

where $N(\alpha, \beta)$ stands for the number of events in which the observables A and B have been found equal to the dichotomic outcomes α and β. Finally we define a parameter which takes into account the correlations for the different observables.

$$S = E(\mathbf{a}, \mathbf{b}) + E(\mathbf{a}', \mathbf{b}) + E(\mathbf{a}, \mathbf{b}') - E(\mathbf{a}', \mathbf{b}') \tag{8}$$

Assuming a local realistic theory CHSH found that the relation $|S| \leq S_{CHSH} = 2$ holds.

To carry out a non-locality test in the Micro-macro” regime, we define the two sets of dichotomic observables for A and B which can be measured over different polarization basis sets. Both partners perform measurements in equatorial basis $\left\{\overrightarrow{\pi}_\phi, \overrightarrow{\pi}_\phi^\perp\right\}$. A associates to the detection of the 2-photons with polarization $\overrightarrow{\pi}_\phi$, i.e. of $\left|2\phi\right\rangle_A$, the observable +1 and to the detection of the 2-photons with polarization $\overrightarrow{\pi}_{\phi\perp}$, i.e. of $\left|2\phi^\perp\right\rangle_A$, the observable -1. The two possible output values $\{\mathbf{a}, \mathbf{a}'\}$ correspond to $\phi_a = \frac{\pi}{4}$ and $\phi_a' = -\frac{\pi}{4}$: Figure 7-**b**.

B associates to the detection of the $\left|\Phi^{2\phi}\right\rangle_B$ the observable +1 and to the detection of the $\left|\Phi^{2\phi\perp}\right\rangle_B$ the observable -1. The two possible values $\{\mathbf{b}, \mathbf{b}'\}$ correspond to $\phi_b = 0$ and $\phi_b' = \frac{\pi}{2}$. In order to achieve a high discrimination among $\left\{\left|\Phi^{2\phi}\right\rangle_B, \left|\Phi^{2\phi\perp}\right\rangle_B\right\}$ the OF-filter is adopted.

Let us consider briefly the conceptual issues and the possible loopholes raised by the present nonlocality test. As shown in Figure 7, our system fully reproduces the

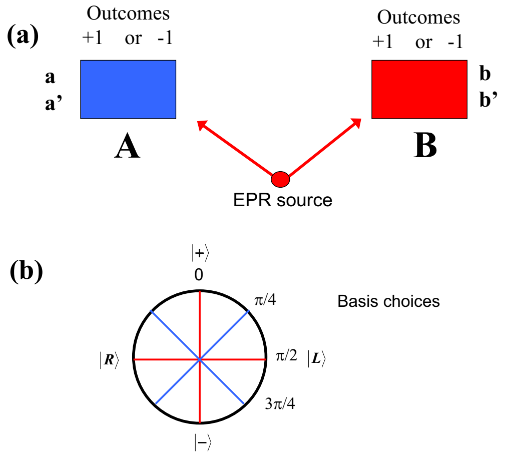

FIG. 7: (**a**) Conceptual scheme for testing the Bell-CHSH nonlocality Test. (**b**) Settings of the ϕ phases by which the Bell-CHSH test was carried out.

standard Bohm-Bell scheme for testing nonlocality for an entangled pair of spin-1 particles [35]. Two space-like separated, uncorrelated "black boxes" A and B receive the entangled photons from a common EPR source, i.e. involving the NL crystal 1 (C1). The box A coincides with the "ALICE Box" in Figure 2 while the box B contains all measurement devices appearing in the"BOB Box" in Figure 2 and the QI-OPA amplifier, i.e. the NL crystal 2 (C2). Assuming this interpretation, the following two conditions characterize our present nonlocality test: (1) No artificial selection, sampling or filtering whatsoever is made on the photon couples emitted by the EPR source, before the particles enter the boxes A and B. (2) Any external operation acting on the particles before measurement, e.g. amplification, loss due to reduced quantum efficiencies, OF-filtering etc., is a "local operation" because it is exclusively attributable to the separated internal dynamics of the devices contained in the boxes A and B. On the basis of these premises any sampling or filtering made on the particles by our system must be defined a "fair sampling" operation [3]. There "fairness" is precisely implied by condition (1), i.e. stating that no externally biased perturbation is allowed to act on the only carriers of nonlocality connecting A and B : the EPR entangled particles. On these premises, any hidden variable analysis of the overall process will possibly identify new "loopholes" in our test. Certainly the simple "detection loophole" does not apply to our complex scheme [36]. In this connection, we remind that several non-locality tests valid for post-selected events have been conceived in the past. For instance, the ones adopting photonic GHZ states [37] or 4 photon cluster states [38], in which the tripartite entangled state is generated only when a detector fires on each output mode. We believe that our test is similar to the last condition, the only difference being due to the use made in either cases by the local post-selection operation. While in the previous case it was instrumental to generate a quantum state, in our case it is used to properly improve a local measurement procedure, i.e. to make the quantum measurement sharper. A procedure somewhat similar to ours was adopted by Babichev et al. to carry out the non-locality proof of single photon dual-mode optical qubit [39]. We believe that a careful quantum analysis will be required to fully clarify the aspects of our POVM method in the context of any hidden variable theory [40, 41].

Experimentally we obtained the following values by carrying out a measurement with a duration of 4 hours and a statistics per setting equal to about 500 events:

$E(\phi_a, \phi_b)$	$E(\phi'_a, \phi_b)$	$E(\phi_a, \phi'_b)$	$E(\phi'_a, \phi'_b)$
0.643 ± 0.027	0.551 ± 0.029	0.608 ± 0.017	-0.453 ± 0.023

which leads to

$$S = 2.256 \pm 0.049$$

Hence a violation by more than 5 standard deviation over the value $S_{CHSH} = 2$ is obtained. This experimental value is in agreement with an average experimental visibility of $V \sim 80\%$ which should lead to $S = 2.26$.

III. APPLICATIONS TO QUANTUM INFORMATION. MACRO-MACRO ENTANGLEMENT

We have experimentally demonstrated the quantum non-separability of a Micro-Macro-system. Furthermore, by increasing the size of the injected "seed" state, namely by adopting at the outset a 4-photon entangled state, we have reported a violation of Bell inequalities. It is possible to demonstrate that the methods adopted in present experiment can be re-formulated in the context of the "continuous variable" approach (CV), which is commonly used to analyze the quantum informational content of "quadrature operators" for multi-particle systems [42]. Indeed the intersection of the present QI-OPA method and of the CV approach appears to be an insightful and little explored field of research to which the present work will contribute by eliciting an enlightening theoretical endeavor. However, in spite of these appealing perspectives, we believe that the QI-OPA approach is more directly applicable to the field of Quantum Information and Computation in virtue of the intrinsic *information-preserving* property of the QI-OPA dynamics. Indeed, this property implies the direct realization of the quantum map $(\alpha \left|\phi\right\rangle + \beta \left|\phi^{\perp}\right\rangle) \longrightarrow (\alpha \left|\Phi^{\phi}\right\rangle + \beta \left|\Phi^{\phi\perp}\right\rangle)$ connecting any single-particle qubit to a corresponding Macro-qubit, by then allowing the direct extension to the multi particle regime of most binary logic methods and algorithms. A simple example may be offered by the implementation of several universal 2-qubit logic gates such as the CNOT or the phase-gate. Consider a 2-qubit phase gate in which the control-target interaction is provided by a Kerr-type optical nonlinearity. It is well known that

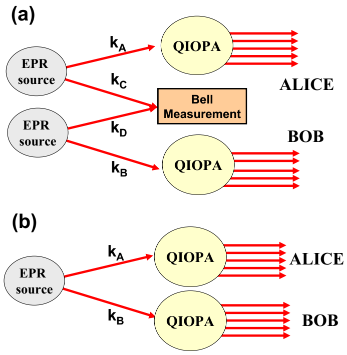

FIG. 8: Implementation of Macro-Macro entanglement (a) via two QI-OPA entanglement swapping (b) through two optical parametric amplifiers.

the strength of this nonlinearity is far too small to provide a sizable interaction between the"control" and the "target" single-particle qubits, even in the special case of the atomic quasi resonant electromagnetic induced transparency configuration (EIT) [43, 44]. However, by replacing these qubits by the corresponding Macro-qubits associated with N photons, the NL interaction strength can be enhanced by a large factor χ since the 3d-order NL polarization scales as $N^{3/2}$. By assuming the values of the NL gain g realized experimentally in the present work, the value of this factor can be as large as $\chi \approx 10^7$ for $g = 4.4$ and $\chi \approx 10^{11}$ for $g = 6.0$. Such large enhancement of the NL interaction strength may represent the key solution towards the technical implementation of the most critical optical components of a quantum computer.
Of course, all these applications are made possible by an important property of the QI-OPA scheme: there the multi-particle entangled Macro-states are *directly accessible* at the output of the QI-OPA apparatus. In other words, in our systems the many photons involved in the quantum superpositions are not sealed or trapped in hardly accessible electromagnetic cavities, nor suffer from decoherence processes due to handling, storing or measurement procedures.

At last, the Micro-Macro experimental method demonstrated in this work can be upgraded in order to achieve an entangled Macro-Macro system showing again marked nonlocality features. Such scheme could exploit an "entanglement swapping" protocol [45] as shown in Fig.8-(**a**). There the final entangled state is achieved through a standard intermediate Bell measurement carried out on the Micro-states. A similar process has been suggested in different contexts, for instance to entangle micromechanical oscillators [46]. As an alternative approach, the single photon states on mode $\mathbf{k}_A$ and $\mathbf{k}_B$ could be amplified by two independent QI-OPA's :Fig.8-(**b**). Another appealing perspective is the light-matter entanglement, consisting of the coupling, either linear or nonlinear, of the multi-photon generated QI-OPA fields with the mechanical motion of atomic systems. As an example, the coupling of a Bose Einstein Condensed (BEC) assembly of Rb atoms with the entangled multi-particle field generated by our apparatus is presently being investigated in our Laboratories [47]. All this can open interesting scenarios in modern science and technology. On a very fundamental side, the observation of quantum phenomena with an increasing number of particles can shed light on the elusive boundary between the "classical" and the "quantum" worlds, and provide new paths to investigate the notion of quantum wavefunction and its intriguing "collapse" [48].

Acknowledgments

We acknowledge technical support from Sandro Giacomini, and Giorgio Milani and experimental collaboration with Eleonora Nagali,Tiziano De Angelis and Nicolo' Spagnolo. This work was supported by the PRIN 2005 of MIUR and project INNESCO 2006 of CNISM.

APPENDIX A: EXPERIMENTAL SETUP

We provide here more structural details on the apparatus shown in Figure 2 of the main text (MT) . The excitation source was a Ti:Sa Coherent MIRA mode-locked laser amplified by a Ti:Sa regenerative REGA device operating with pulse duration $180fs$, repetition rate $250kHz$ and average output power: $1.6\,W$. The pumping laser of the amplifier was a laser Coherent Verdi operating at a continuous-wave $13.5W$ power level . The output beam, frequency-doubled by second-harmonic generation, provided the OPA excitation field beam at the UV wavelength (wl) $\lambda_P = 397.5nm$ with power: $750 \div 800mW$. The UV beam, splitted in two beams through a $\lambda/2$ waveplate (wp) and a polarizing beam splitter (PBS), excited two BBO (β-barium borate) NL crystals cut for type II phase-matching. Crystal 1, (C1) excited by the beam $\mathbf{k}_P$, was the SPDC source of entangled photon couples with wl $\lambda = 2\lambda_P$, emitted over the two output modes $\mathbf{k}_j$ $(j = A, B)$ in the *singlet* state $|\Psi^-\rangle_{A,B}$=$2^{-1/2}\left(|H\rangle_A |V\rangle_B - |V\rangle_A |H\rangle_B\right)$. The power of beam $\mathbf{k}_P$ was set at a low enough level to generate with negligible probability more than two simultaneous pairs of photons. The photon associated with mode $\mathbf{k}_A$, hereafter referred to as *trigger* mode, was coupled into a single mode fiber and excited through a PBS one of the single photon counting modules (SPCM) (D_A, D_A^*), while the single photon state generated over the mode $\mathbf{k}_B$ was injected, together with a strong UV pump beam (mode $\mathbf{k}'_P$), into the NL crystal 2 (C2) and stimulated the simultaneous emission of large number of photon pairs. The measurement was carried out on the mode $\mathbf{k}_A$ by adopting a set of two waveplates, $\lambda/2 + \lambda/4$, a Soleil-Babinet variable phase-shifter (PS) and a polarizing beam-splitter PBS. By a delay (Z) the time superposition in the OPA of the excitation UV pulse and of the injection photon wavepacket was provided. The injected single photon and the UV pump beam $\mathbf{k}'_P$ were superimposed by means of a dichroic mirror (DM) with high reflectivity at λ and high transmittivity at λ_P. The output state of the crystal 2 with wl λ was spatially separated by the fundamental UV beam again by a dichroic mirror (DM) and spectrally filtered by an interference filter (IF) with bandwidth $\Delta\lambda = 1.5nm$, transmittivity ($\approx 80\%$) and coupled to a single mode fiber (SM), polarization analyzed and then detected by 2 equal photomultipliers (PM) P_B and P_B^* . The SPCM detectors were single-photon modules Perkin Elmer type AQR14-FC. The PM's were Burle A02 with a Ga-As photocathode having a detector quantum efficiency $\eta_{QE}^D = 13\%$.

In a first experiment with no quantum injection, we measured the gain value g of the optical parametric process and the overall detection efficiency η_{QE} of the detection apparatus. The average signal amplitude of P_B was measured for different values of the UV power. The gain value g of the process was obtained by fitting the experimental data [29, 30] with an exponential function, leading to $g_{\max} = (4.40 \pm 0.02)$, corresponding to an overall mean photon number per mode $\overline{m} = 1470$. A gain $g = 6.0$, $\overline{m} = 4.0 \times 10^4$ was also realized with no substantial changes in the apparatus. The exponential growth demonstrates the multiple generation of photon pairs by a self-stimulation process within the NL crystal. The overall efficiency on the $\mathbf{k}_B$ mode, $\eta_B \simeq 3\%$ was determined by fiber coupling ($\sim 50\%$), IF transmittivity and detector η_{QE}^D.

1. Orthogonality Filter

Here we give more details of the "Orthogonality filter" (OF), a device adopted to discriminate among the quantum states $\{|\Phi^{\pm}\rangle_B\}$. This operation is realized by exploiting the different functional characteristics existing between the corresponding photon number distribution patterns $P^+(m,n)$ and $P^-(m,n)$ corresponding to the Macro states expressed respectively by Equations(2-3) of MT for $\phi = 0$ and $\phi = \pi$: $|\Phi^+\rangle_B$ and $|\Phi^-\rangle_B$. Precisely, since the single-photon resolving detection is beyond the reach of present technology and $\eta_{QE}^D < 1$, we may consider that the two Fock components of the Macro states, $|(2i+1)+;(2j)-\rangle$ and $|(2i)+;(2j+1)-\rangle$ belonging respectively to the expressions of $|\Phi^+\rangle_B$ and $|\Phi^-\rangle_B$, generate the same signals at the output of any couple of PM detectors: $(I_+, I_-) \propto (m \approx 2i,\ n \approx 2j)$. However a discrimination may still be carried out efficiently between the above orthogonal Macro states by exploiting the different "shape" of the probability distributions $P^+(m,n)$ and $P^-(m,n)$ for large values of $|n-m|$. For this purpose, we introduce an appropriate threshold $k > 0$ for signal discrimination. By analyzing the two probability distributions we infer that when $(m-n) > k$ the signals (I_+, I_-) can be attributed to the state $|\Phi^+\rangle_B$ with a fidelity that increases with the value of k. In this case the measured eigenvalue of $\widehat{\Sigma}_3^B$ is found $= +1$. Likewise, when $(n-m) > k$ the signals (I_+, I_-) is inferred to correspond to the state $|\Phi^-\rangle_B$ with $\widehat{\Sigma}_3^B$ eigenvalue = -1. The events which satisfy the inequality $-k < (m-n) < k$ are discarded since there the two distributions approximately overlap impairing a reliable state discrimination. This technique can be adopted even with a low value of detection efficiency ($\eta \simeq 10^{-2}$) since it is found that the functional characteristics of the distributions $P^{\pm}(m,n)$ which are pertaining to the discrimination of the states $|\Phi^{\pm}\rangle_B$ are preserved under the signal propagation over a lossy channel. This important point has been carefully investigated theoretically and experimentally in our laboratory [27].

The measurement scheme just described has been physically implemented by the OF shown in Figure 9, an electronic device by which the pulse heights of the couple of input signals (I_+, I_-) provided by two PM's (P_B, P_B^*) are summed with opposite signs by a balanced linear amplifier (LA) with "gain" G (chip National LM733). Each of the two signals $\pm[G(I_+ - I_-)] \equiv \pm[G\xi(m-n)]$ realized at the two symmetric outputs of (LA) feeds an independent electronic discriminator (AD9696) set at a common threshold level $G\xi k$. Owing to previous considerations the two discriminators never fire simultaneously and each of them provides, when activated, a standard transistor-transistor-logic (TTL) square signal at its output port. As said, when the condition $(I_+ - I_-) > \xi k$, i.e.

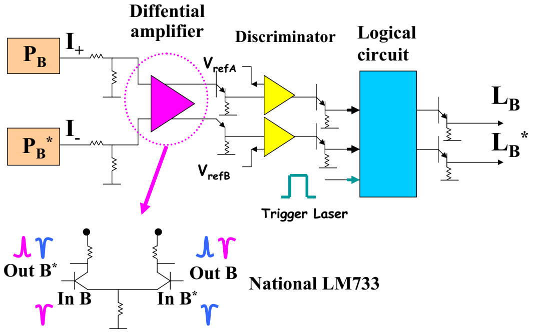

FIG. 9: Electronic Orthogonality filter OF. The electronic signals (I_+, I_-) emitted simultaneously by two photomultipliers P_B and P_B feed a linear difference amplifier (National LM733). Each of the two output ports of the amplifier is connected to an electronic discriminator set at a threshold level $\xi k > 0$ equal for the two discriminators. Each discriminator emits a TTL electronic square signal if the threshold is overcome by the difference signals. Precisely, a TTL signal is realized at the port L_B when: $(I_+ - I_-) > \xi k$ or at the port L_B^* when $(I_- - I_+) > \xi k$. The two discriminators never fire simultaneously. The rejected events, for $-\xi k < (I_+ - I_-) < \xi k$, correspond to the "inconclusive outcomes" of our generalized POVM measurement technique.

$(m-n) > k$ is satisfied, a TTL signal L_B is generated and then the realization of the state $|\Phi^+\rangle_B$ is inferred. Likewise, when $(I_- - I_+) > \xi k$ a TTL signal L_B^* is generated and the realization of the state $|\Phi^-\rangle_B$ is inferred. The events that are discarded for: $-\xi k < (I_+ - I_-) < \xi k$ correspond to the "inconclusive" outcomes of any POVM [31].

The OF device has been tested and characterized in condition of spontaneous emission, i.e., in absence of any quantum injection into C2. In this condition the output TTL signals $L_B(L_B^*)$ were measured by sending only the signal $I_+(I_-)$ as input and by varying the threshold k. In this regime the number of photons generated per mode should exhibit a thermal probability distribution: $P(n) = \frac{\langle n\rangle^n}{(1+\langle n\rangle)^{n+1}}$ with $\langle n\rangle$ average photon number per mode. Hence the probability to detect a signal above the threshold k is: $\Pi(k) = \sum_{n=k}^{\infty} P(n) = \left(\frac{\langle n\rangle}{(1+\langle n\rangle)}\right)^k$. We have experimentally checked the dependence on the threshold k of the number of counts, which is expressed by $R \times \Pi(k)$, being R the repetition rate of the source. The experimental data shown by Figure 10 represent a fair support of the expected exponential behavior.

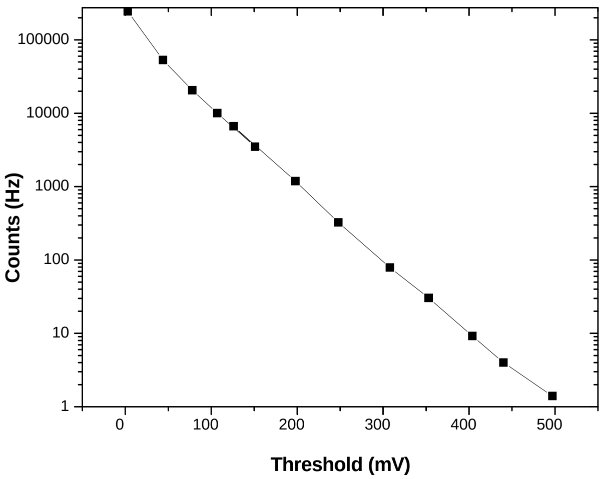

FIG. 10: Count rates versus the threshold k. The measured average electronic signal was $\simeq 40mV$, while the repetition rate of the main laser source was 250 kHz.

2. Entanglement Test

To carry out the measurement of the degree of the entanglement ALICE and BOB adopt a common polarization basis i. In the basis $\{\overrightarrow{\pi}_+, \overrightarrow{\pi}_-\}$ the measurements were carried out by setting the $\frac{\lambda}{4}$ and $\frac{\lambda}{2}$ waveplates, shown in the ALICE Box in Figure 2, with the optical axes making angles respect to the vertical direction equal to 45° and 22.5°, respectively. An identical setting was adopted for the $\frac{\lambda}{4}$ and $\frac{\lambda}{2}$ wp's in the BOB Box in Figure 2. Likewise, in the basis $\{\overrightarrow{\pi}_R, \overrightarrow{\pi}_L\}$ the measurements were carried out by setting the two sets of $\frac{\lambda}{4}$, $\frac{\lambda}{2}$ wp's, shown in the ALICE and BOB Boxes, with the optical axes making identical angles respect to the vertical 0° and 22.5°, respectively. The phase shifter (PS), placed at the ALICE's site, consisted of a Soleil-Babinet compensator, i.e. a variable birefringent retarder.

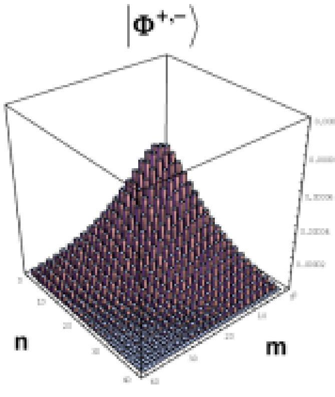

FIG. 11: Theoretical photon number probability distribution $P^{\pm}(m,n)$ for the Macro-state: $|\Phi^{+,-}\rangle$ $(g = 1.5)$.

The experimental "Visibility" V_i were measured by recording the coincidence patterns $\{[L_B, D_A], [L_B^*, D_A], [L_B, D_A^*], [L_B^*, D_A^*]\}$ recorded for both spaces A and B in the basis i [30]. According to the standard definition: $V_i = (I_{\max} - I_{\min})/(I_{\max} + I_{\min})$ where $I_{\max}, I_{\min}$ are respectively the maximum and the minimum values of the detected signals corresponding to the value of phase $\phi = 0$. The visibility values reported in the Main Text were recorded by averaging over a time $\simeq 5$ hours the results of 4000 events for each experimental datum shown in Figure 4, for each basis.

It$'$s worth noting that the above procedure is "phase covariant", i.e. the overall quantum efficiency of the electronic filter OF is independent of the phase ϕ. In other words, and most important in the present context, every state produced by QIOPA, $\left|\Phi^{\phi}\right\rangle_B = \widehat{U}\left|\phi\right\rangle_B$, has the same overall probability to be filtered by the electronic filter and to produce a TTL signal at one output port, either L_B or L_B^*. This feature was experimentally verified by measuring the OF-filtering probability P_{fil} for different phase values of the injected qubit. In particular, P_{fil} assumes the same value when the measurement is applied to the state $\{|\Phi^+\rangle_B, |\Phi^-\rangle_B\}$ and $\{\left|\Phi^R\right\rangle_B, \left|\Phi^L\right\rangle_B\}$ states.

3. CHSH tests

Let us now account for the non-locality test by considering the measurement carried out within the two Boxes A and B shown in Figure 7. (A) *Measurement at the A Box.* The angles respect to the vertical made by the optical axes of the waveplates $\frac{\lambda}{4}, \frac{\lambda}{2}$ shown in the ALICE Box in Figure 2 were set at 0° and 22.5°, respectively. The phase shifter (PS) was set in two different positions to obtain $\phi_a = \frac{\pi}{4}$ and $\phi'_a = -\frac{\pi}{4}$. (B) *Measurement at the B Box.* The basis corresponding to $\phi_b = 0$ was obtained by setting the angles respect to the vertical made by the optical axes of the wp's $\frac{\lambda}{4}, \frac{\lambda}{2}$ shown in the BOB Box in Figure 2, at the values 45° and 22.5°, respectively. The basis corresponding to $\phi'_b = \frac{\pi}{2}$ was obtained by setting the angles respect to the vertical made by the optical axes of the same wp's $\frac{\lambda}{4}, \frac{\lambda}{2}$ at the values 0° and 22.5°, respectively. As shown in Figure 2, in the B Box the above phase changes were made by acting on the Macro-states, i.e., on the output multi-particle beam emerging from the QI-OPA.

APPENDIX B: 2-PHOTON WAVEFUNCTION

The Macro-state generated by QI-OPA on mode k_B when a 2-photon state $|(2)\pm\rangle_B$ is injected, is expressed by

$$\left|\Phi^{2\pm}\right\rangle_B = -\frac{\Gamma}{C\sqrt{2}} \sum_{i,j=0}^{\infty} \gamma_{ij} \frac{\sqrt{(2i)!(2j)!}}{i!j!} \left|(2i)\pm;(2j)\mp\right\rangle_B + \frac{1}{C^3} \sum_{i,j=0}^{\infty} \gamma_{ij} \frac{\sqrt{(2i+2)!(2j)!}}{i!j!} \left|(2i+2)\pm;(2j)\mp\right\rangle_B \tag{B1}$$

While, the following Macro-state is generated if a state $|1+;1-\rangle$ is injected:

$$\left|\Phi^{+,-}\right\rangle_B = \frac{1}{C^3} \sum_{i,j} (-1)^j \left(\frac{\Gamma}{2}\right)^{i+j} \frac{\sqrt{(2i+1)!\,(2j+1)!}}{i!j!} \left|(2i+1)+;(2j+1)-\right\rangle_B \tag{B2}$$

The photon number probability distribution for the Macro-state $|\Phi^{+,-}\rangle_B$ is reported in Figure 11.

[1] Einstein, A., Podolsky,B., & Rosen, N., Can Quantum-Mechanical Description of Physical Reality Be Considered Complete? , *Phys. Rev.* **47**, 777-780 (1935).

[2] Schroedinger, E., *Naturwissenschaften* **23**, 807812, 823 828, 844849 (1935). English translation 1983 in Quantum Theory and Measurement, edited by J. A. Wheeler and W. H. Zurek (Princeton University, Princeton, NJ), p. 152.

[3] Bell, J.S., Physics (Long Island, N.Y.) **1**, 195 (1965); Clauser, J.F., Horne M.A., Shimony, A., & Holt, R.A., Proposed Experiment to Test Local Hidden-Variable Theories, *Phys. Rev. Lett.* **23**, 880 (1969); Aspect, A., Grangier, P., and Roger, G., Experimental Tests of Realistic Local Theories via Bell's Theorem, *Phys. Rev. Lett.* **47**, 460 (1981).

[4] De Martini, F., et al., Non-linear Parametric Processes in Quantum Information, *Prog. in Quantum Electronics* **29**, 165-256 (2005).

[5] Zurek, W.H., Decoherence, einselection, and the quantum origins of the classical, *Rev. Mod. Phys.* **75**, 715-775 (2003); Schlosshauer, M., Decoherence, the measurement problem, and interpretations of quantum mechanics, *Rev. Mod. Phys.* **76**, 1267-1305 (2005).

[6] Kwiat, P.G., et al., New high-intensity source of polarization-entangled photon pairs, *Phys. Rev. Lett.* 75, 43374341 (1995).

[7] Blinov,B.B., Moehring, D.L., Duan, L.-M. , & Monroe, C., Observation of entanglement between a single trapped atom and a single photon, *Nature (London)* 428, 153-157 (2004).

[8] Volz, J., et al., Observation of Entanglement of a Single Photon with a Trapped Atom, *Phys. Rev. Lett.* **96**, 030404 (2006).

[9] Matsukevich, D. N. , et al., Entanglement of a Photon and a Collective Atomic Excitation, *Phys. Rev. Lett.* **95**, 040405 (2005).

[10] de Riedmatten, H., et al., Direct Measurement of Decoherence for Entanglement between a Photon and Stored Atomic Excitation, *Phys. Rev. Lett.* **97**, 113603 (2006)

[11] Matsukevich, D.N., et al., Entanglement of Remote Atomic Qubits , *Phys. Rev. Lett.* **96**, 030405 (2006).

[12] Lan, S.Y. et al., Dual-Species Matter Qubit Entangled with Light, *Phys. Rev. Lett.* **98**, 123602 (2007)

[13] Julsgaard, B., Kozhekin, A., & Polzik, E.S., Experimental long-lived entanglement of two macroscopic objects, *Nature* **413** 400-403 (2001).

[14] Moehring, et al., Entanglement of single-atom quantum bits at a distance, *Nature(London)***449**, 68-71 (2007).

[15] Chou, C. W., et al., Measurement-induced entanglement for excitation stored in remote atomic ensembles, *Nature* **438**, 828-832 (2005).

[16] Berkley, A.J., et al., Entangled macroscopic quan-

tum states in two superconducting qubits (phase qubit), www.sciencexpress.org/15 May 2003/Page 1/10.1126/science.1084528.

[17] Pan, J.-W., et al. Experimental demonstration of four-photon entanglement and high-fidelity teleportation, *Phys. Rev. Lett.* **86**, 44354438 (2001).

[18] Zhao, Z., et al., Experimental demonstration of five-photon entanglement and open-destination teleportation, *Nature (London)* **430**, 5458 (2004).

[19] Leibfried, D., et al., Creation of a six-atom 'Schrdinger cat' state, *Nature (London)* 438, 639642 (2005).

[20] Lu, C.-Y., et al., Experimental entanglement of six photons in graph states, *Nature Physics* **3**, 91-95 (2007).

[21] Halder, M., et al., Entangling independent photons by time measurement, *Nature Physics* **3**, 692-695 (2007).

[22] De Martini, F., Amplification of Quantum Entanglement, *Phys. Rev. Lett.* **81**, 2842-2845 (1998); De Martini, F., Quantum Superposition of Parametrically Amplified Multiphoton Pure States, *Phys. Lett. A* **250**,15-19 (1998).

[23] Pelliccia, D., Schettini, V., Sciarrino, F., Sias, C. & De Martini, F., Contextual realization of the universal quantum cloning machine and of the universal-not gate by quantum-injected optical parametric amplification, *Phys. Rev. A* **68**, 042306 (2003); De Martini, F., Pelliccia, D., & Sciarrino, F., Contextual, Optimal, and Universal Realization of the Quantum Cloning Machine and of the NOT Gate. *Phys. Rev. Lett.* **92**, 067901 (2004).

[24] De Martini, D., Sciarrino, F., & Secondi, V., Realization of an Optimally Distinguishable Multiphoton Quantum Superposition, *Phys. Rev. Lett.* **95**, 240401 (2005).

[25] De Martini, F., Buzek, V., Sciarrino, F., & Sias, C., Nature (London) **419**, 815 (2002).

[26] De Angelis, T., Nagali, E., Sciarrino F., & De Martini, F., Experimental test of the no-signaling theorem, *Phys. Rev. Lett.* **99**, 193601 (2007).

[27] Nagali, E., De Angelis, T., Sciarrino, F., & De Martini, F., Experimental realization of macroscopic coherence by phase-covariant cloning of a single photon, *Phys. Rev. A* **76**, 042126 (2007).

[28] Schleich, W.P., Quantum Optics in Phase Space (Wiley, New York, 2001), Chaps. 11 and 16.

[29] Caminati, M., De Martini, F., Perris, R., Sciarrino, F., & Secondi, V., Entanglement, EPR correlations and mesoscopic quantum superposition by the high-gain quantum injected parametric amplification, *Phys. Rev. A* **74**, 062304 (2006).

[30] Eisenberg, H.S.,Khoury, G., Durkin, G.A., Simon, C., & Bouwmeester, D., Quantum Entanglement of a Large Number of Photons, *Phys. Rev. Lett.* **93**, 0193901 (2004); Durkin, G.A., Ph.D. Thesis, Light & Spin Entanglement (2004).

[31] A. Peres, Quantum Theory: Methods and Concepts (Kluwer Academic Publishers, Dordrecht,1995).

[32] Bennett, C.H., Di Vincenzo, D.P:, Smolin, J.A., & Wootters, W.K:, Mixed-state entanglement and quantum error correction, P*hys. Rev. A* **54**, 3824-3851 (1996).

[33] Hill, S. & Wootters, W.K., Entanglement of a pair of quantum bits, *Phys. Rev. Lett.* **78**, 5022-5025 (1997).

[34] Reid, M.D., Munro, W.J., & De Martini, F., Violation of multiparticle Bell inequalities for low- and high-flux parametric amplification using both vacuum and entangled input states, *Phys. Rev. A* **66**, 033801 (2002).

[35] Howell, J.C., Lamas-Linares, A., & Bouwmeester, D., Experimental Violation of a Spin-1 Bell Inequality Using Maximally Entangled Four-Photon States, *Phys. Rev. Lett.* **88**, 030401 (2002)

[36] Kwiat, P. et al., Proposal for a loophole-free Bell inequality experiment, *Phys. Rev. A* **49**, 3209 (1994)

[37] Bouwmeester,D., et al., Observation of Three-Photon Greenberger-Horne-Zeilinger Entanglement, *Phys. Rev. Lett.* **82**, 1345 (1999)

[38] Kiesel, CN., et al., Experimental Analysis of a Four-Qubit Photon Cluster State, *Phys. Rev. Lett.* **95**, 210502 (2005)

[39] Babichev, S.A., Appel, J., & Lvovsky, A.I., Homodyne Tomography and Characterization and Nonlocality of a Dual-Mode Optical Qubit, *Phys. Rev. Lett.* **92**, 0193601 (2004).

[40] Pearle, P., Hidden-Variable Example Based upon Data Rejection, *Phys. Rev. D* **2**, 1418 - 1425 (1970)

[41] Huelga, S.F. , Ferrero, M. & Santos, E., Loophole-free test of the Bell inequality, *Phys. Rev. A* **51**, 5008 (1995)

[42] Braunstein, S.L., & and Loock, P.v., Quantum information with continuous variables, *Rev. Mod. Phys.* **77**, 513 (2005)

[43] Hau, L.V., Harris, S E., Dutton, Z, & Behroozi, C.H., Light speed reduction to 17 metres per second in an ultracold atomic gas, *Nature (London*) 397, 594 (1999).

[44] Fleischhauer, M., Imamoglu, A., &, Marangos J.P., Electromagnetically induced transparency: Optics in coherent media, *Rev. Mod. Phys.* **77**, 633-673 (2005).

[45] Pan, J., et al., Experimental Entanglement Swapping: Entangling Photons That Never Interacted, *Phys. Rev. Lett.* **80**, 3891-3894 (1998).

[46] Pirandola, S., et al., Macroscopic Entanglement by Entanglement Swapping, *Phys. Rev. Lett.* **97**, 150403 (2006).

[47] Cataliotti, F., & De Martini, F., Macroscopic quantum entanglement in light reflection from Bose-Einstein Condensates, (in preparation).

[48] Guerlin, C., et al., Progressive field-state collapse and quantum non-demolition photon counting, *Nature (London)* **448**, 889-893 (2007).